electronics

MDPI

Article

A 3D Coverage Method Involving Dynamic Underwater Wireless Sensor Networks for Marine Ranching Monitoring

Lei Fu [1,2] and Ji Wang [1,2,*]

[1] College of Electronic and Information Engineering, Guangdong Ocean University, Zhanjiang 524088, China; 2112210003@stu.gdou.edu.cn
[2] Guangdong Engineering Technology Research Center of Intelligent Ocean Sensor Network and Equipment, Zhanjiang 524088, China
* Correspondence: wangji@gdou.edu.cn

Abstract: In view of the poor adaptability and uneven coverage of static underwater wireless sensor networks (UWSNs) to environmental changes and the need for dynamic monitoring, a three-dimensional coverage method involving a dynamic UWSNs for marine ranching, based on an improved sparrow search algorithm (ISSA), is proposed. Firstly, the reverse learning strategy was introduced to generate the reverse sparrow individuals and fuse with the initial population, and the individual sparrows with high fitness were selected to improve the search range. Secondly, Levy flight was introduced to optimize the location update of the producer, which effectively expanded the local search capability of the algorithm. Finally, the Cauchy mutation perturbation mechanism was introduced into the scrounger location to update the optimal solution, which enhanced the ability of the algorithm to obtain the global optimal solution. When deploying UWSNs nodes, an autonomous underwater vehicle (AUV) was used as a mobile node to assist the deployment. In the case of underwater obstacles, the coverage hole in the UWSNs was covered by an AUV at specific times. The experimental results show that compared with other algorithms, the ISSA has a shorter mobile path and achieves a higher coverage rate, with lower node energy consumption.

Keywords: marine ranching; underwater wireless sensor networks; sparrow search algorithm; autonomous underwater vehicle; underwater path planning

check for updates

Citation: Fu, L.; Wang, J. A 3D Coverage Method Involving Dynamic Underwater Wireless Sensor Networks for Marine Ranching Monitoring. *Electronics* **2024**, *13*, 4536. https://doi.org/10.3390/electronics13224536

Received: 28 October 2024
Revised: 14 November 2024
Accepted: 15 November 2024
Published: 19 November 2024

Copyright: © 2024 by the authors. Licensee MDPI, Basel, Switzerland. This article is an open access article distributed under the terms and conditions of the Creative Commons Attribution (CC BY) license (https://creativecommons.org/licenses/by/4.0/).

1. Introduction

Wireless sensor networks (WSNs) are composed of sensor nodes deployed in the monitoring area, which form a multi-hop self-organizing network system through wireless communications. They are widely used in military, health, environment, animal and plant, industrial and urban fields [1]. The ocean is one of the most extensive ecosystems on Earth, boasting rich biodiversity and immense resource potential. Marine ranching is an important form of marine resource utilization, which provides humans with abundant food resources by cultivating and breeding aquatic organisms in the ocean [2]. Therefore, to ensure the sustainable operation and ecological balance of marine ranching, underwater wireless sensor networks (UWSNs) are employed to conduct comprehensive and in-depth monitoring of the marine environment [3].

In traditional monitoring of the marine environment, sensor nodes are statically deployed. The dynamic changes in the network caused by water flow lead to coverage holes in the network. The nodes in a dynamic UWSNs are composed of fixed nodes and mobile nodes, and the nodes have mobility. They can adapt to the dynamic underwater environment. A dynamic UWSNs utilizes autonomous underwater vehicle (AUV) as mobile nodes to precisely cover target areas, thus mitigating the limitations of traditional fixed deployment [4,5]. In addition, swarm intelligence technology, with its characteristics of decentralization, high intelligence, and flexibility, has been widely applied in regard to marine exploration equipment, such as UWSNs, AUV, and unmanned surface vessels

(USVs). This technology has significantly enhanced the efficiency of marine exploration and development, and has adapted to the changing marine environment [6–11].

In terms of traditional coverage strategies for terrestrial WSNs, two-dimensional (2D) planar coverage was mostly adopted and the research in this area has tended to be well-developed [12–14]. Qu et al. [15] proposed a coverage optimization approach for WSNs using the improved multi-strategy grey wolf optimizer (IGWO-MS) to address the two specific challenges of increased node deployment costs and insufficient effective coverage by WSNs. Chang et al. [16] proposed a variant of the tuna swarm optimization algorithm (TSO), called SITSO, based on behavioral evaluation and a simplex strategy, and applied the algorithm to the 2D WSNs coverage optimization problem. However, the deployment environment for UWSNs in marine ranching is drastically different, involving a complex and dynamic underwater three-dimensional (3D) space. This characteristic presents both novel challenges and opportunities for environmental monitoring and resource management in marine ranching. Zhang et al. [17] introduced a reinforced drosophila optimal algorithm to adapt and make the positioning of mobile nodes more efficient, thereby improving the coverage rate of a 3D UWSNs. Priyadarshi et al. [18] introduced a cube-based 3D coverage model, refined its deployment configuration to maximize coverage and established a correlation between the radius of the sensor nodes and the achieved coverage rate. Yu et al. [19] proposed an adaptive grey wolf optimizer, which was pioneering in terms of enhancing WSNs coverage not only in 2D domains, but also in intricate 3D environments. However, it was deployed in a static environment, where nodes are not mobile. Wang et al. [20] introduced an enhanced virtual force algorithm, which leveraged the k-equivalent radius concept to optimize the coverage of a 3D UWSNs. This algorithm established a diversified k-coverage sensor network based on the needs of the sensor nodes to attain uneven regional coverage. Saad et al. [21] presented a 3D environmental coverage pattern using Bresenham's line of sight. The algorithm utilized a multi-objective genetic algorithm, equipped with novel adaptive and guided genetic operators to solve the problem. However, there is still room for improvement in regard to the energy efficiency of the nodes in this model. Luo et al. [22] inspired by the physical effects of water flow, proposed a 3D virtual force underwater sensor network coverage algorithm that considers node mobility. Liu et al. [23] put forward an ingenious and succinct particle swarm optimization algorithm tailored to address coverage obstacles in a 3D WSNs. This algorithm leveraged the pareto distribution to simulate the positioning of the particle swarm, while incorporating a gaussian perturbation approach to efficiently evade local optima. Gou et al. [24] introduced an effective method to enhance coverage based on 3D-Voronoi partitioning and K-means clustering. The method enhanced node uniformity through two rounds of deployment, employing a polynomial mutation strategy.

Currently, most underwater research efforts only consider deployment with immobile nodes, yet nodes in underwater environments exhibit drifting properties, which allow them to move freely. This free-flowing nature can lead to uneven node distribution, affecting the stability of communication between the nodes. Therefore, an AUV-assisted coverage method for a marine ranching UWSNs, based on an ISSA, is proposed. This method aims to improve the feasibility and economics of deploying UWSNs nodes in marine ranching, by fully exploiting the advantages of AUV as mobile nodes and allowing the project implementer to flexibly adjust the configuration ratio of mobile and fixed sensors, according to the specific needs and cost budget to achieve effective coverage of the UWSNs.

The main research-related contributions of this paper are as follows:

1. Mobile and fixed nodes are deployed underwater and the mobile nodes find the best deployment location through the ISSA;
2. After the nodes have been successfully deployed, whenever a node coverage hole occurs in the network, use an AUV to move to the location that needs to be monitored to repair the coverage hole;
3. According to the real underwater environment, avoid fish, sensors, seamounts, and other underwater obstacles, through underwater path planning.

2. Dynamic UWSNs Model for Marine Ranching

Figure 1 illustrates the model of the marine ranching UWSNs, which is centered on efficient and stable underwater communication via acoustic signals. The environmental monitoring platform for marine ranching is comprehensively constructed, encompassing a diverse range of communication devices that span from the depths of the ocean to the land, extending into the sky and to satellites. These devices not only possess communication capabilities, but also have the ability to collect, transmit, and process various environmental data within the marine ranching system in real time, promoting the sustainable development of fishery resources, while ensuring the ecological health of marine ranching. Through this comprehensive monitoring network covering land, sea, air, and space, managers of the marine ranching operation can accurately grasp the changes in the marine environment, enabling them to make scientific decisions, optimize breeding plans, and enhance breeding efficiency. An AUV is used as a mobile node to assist the deployment of UWSNs nodes. The AUV collects environmental data through the sensor system, communicates with the ground station through the communication system, receives task instructions, and autonomously navigates and plans the underwater path, while avoiding obstacles to achieve efficient and autonomous node deployment.

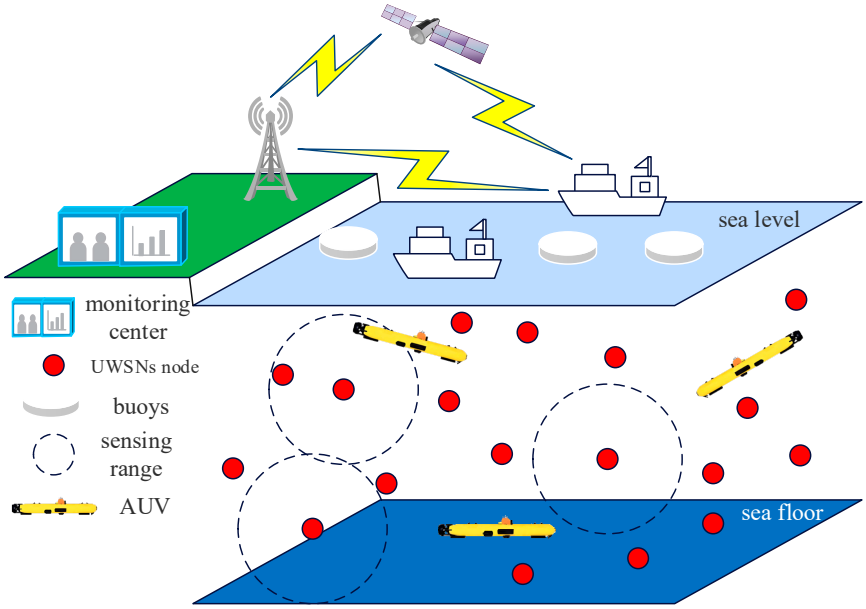


Figure 1. UWSNs model for marine ranching.

2.1. Underwater Area Coverage Model

In the underwater surveillance zone, N sensor nodes have been deployed, with the node set denoted as $S = \{s_1, s_2, s_3, \ldots, s_n\}$, m represents the mobile sensor nodes, while im represents the fixed sensor nodes. The underwater sensing field has been divided into g regions and the set of monitoring points is indicated as $G = (g_1, g_2, g_3, \ldots, g_n)$.

For the purpose of research rationality, the following presumptions are established regarding the UWSNs nodes in the marine ranching scenario:

1. Each sensor node records its position information during deployment;
2. The communication performance of the sensor nodes is stable and unaffected by the water flow. All nodes have a sensing radius R and a communication radius Rc, where $Rc \geq R$;
3. There exist regions within the underwater network that require less intensive monitoring tasks. In cases where coverage holes that affect network operation occur or there are areas that urgently require monitoring, the Sink node can dispatch mobile nodes for weaker monitoring tasks compared to those areas using path planning algorithms.

In the deployment of a sensing field, when the sensing radius R of the sensor nodes n covers the monitoring point g, it achieves complete coverage of that region. The Euclidean distance from the sensor node to the monitoring point is:

$$d(s_i, g_j) = \sqrt{(x_i - x_j)^2 + (y_i - y_j)^2 + (z_i - z_j)^2} \tag{1}$$

Using a Boolean sensing model, if a monitoring point is within the sensing radius R, its sensing degree is recorded as 1, otherwise it is recorded as 0. The sensing probability of monitoring point g_j by sensor node n_i is:

$$P(s_i, g_j) = \begin{cases} 1 & d(s_i, g_j) \leq R \\ 0 & \text{otherwise} \end{cases} \tag{2}$$

In the underwater 3D network consisting of l monitoring points to be surveyed, the collective sensing probability of all the sensor nodes for these surveillance points is defined as:

$$C_p(s_{all}, g_j) = 1 - \prod_{i=1}^{l} (1 - P(s_i, g_j)) \tag{3}$$

To calculate the collective perception likelihood of each monitoring point, Equation (3) is applied, with s_{all} representing the total number of sensor nodes within the observation area. The coverage of l monitoring areas can be obtained from the sum of the joint sensing rate of all the monitoring points, as follows:

$$C_l = \frac{\sum_{i=1}^{n} C_p(s_{all}, g_j)}{l} \tag{4}$$

The total movement distance of each mobile node over the iteration count T is:

$$m_l = \sum_{t=1}^{T-1} \sqrt{(x_t - x_{t+1})^2 + (y_t - y_{t+1})^2 + (z_t - z_{t+1})^2} \tag{5}$$

where t is the present 3D point position; in the subsequent iteration, the next position is designated as $t + 1$.

The underwater energy consumption of the mobile node E_{total} is as follows:

$$E_{total} = e_{km} \cdot \frac{m_l}{1000} \tag{6}$$

where e_{km} represents how many kwh are consumed per kilometer.

2.2. The 3D Underwater Path Planning Model

This paper addresses the optimization problems in terms of the path length, navigation depth, and navigation safety, in constructing an underwater 3D path planning model.

2.2.1. Path Length

Path length is a crucial criterion for assessing the path's quality and short paths help to reduce AUV energy consumption. The path length formula is:

$$P_l = \sum_{i=1}^{n} \sqrt{(x_{i+1} - x_i)^2 + (y_{i+1} - y_i)^2 + (z_{i+1} - z_i)^2} \tag{7}$$

where n represents the number of waypoints and (x_i, y_i, z_i) is the location of the ith waypoint.

2.2.2. Depth of Navigation

In order to ensure the navigational efficiency of the AUV, save energy, and maintain safety, it is particularly important to choose a reasonable navigation depth. In addition, in order to ensure the stealthiness of the AUV during navigation, usually its depth fluctuation cannot be too large, so maintaining stable navigation is crucial. The navigation depth adaptation function is:

$$P_h = \sqrt{\frac{1}{n}\sum_{i=0}^{n-1}(z_i - \overline{z})^2}, \overline{z} = \frac{1}{n}\sum_{i=0}^{n-1} z_i \tag{8}$$

2.2.3. Safety of Navigation

To ensure AUV safety, route planning needs to take into account navigation safety and ensure that the AUV is able to avoid obstacles.

In the underwater environment, there exists an obstacle B, with its center at coordinate O and a radius of R_B. To ensure safety, the AUV needs to maintain a distance D_B from the obstacle that is greater than the safe distance threshold V, to remain outside the radius of obstacle B. Additionally, the AUV must keep a safe distance from obstacle B. The formula for navigational safety is:

$$P_s = \begin{cases} 0, D_B \geq V \\ V - D_B, R_B < D_B < V \\ \infty, D_B < R_B \end{cases} \tag{9}$$

The above three cost functions are weighted and summed up to form the objective function for path planning:

$$P = \omega_1 P_l + \omega_2 P_h + \omega_3 P_s \tag{10}$$

where the path length, trajectory smoothness, and navigation safety correspond to the weighting coefficients ω_1, ω_2, and ω_3, respectively, and a smaller p-value implies a higher level of quality of the chosen path.

3. Sparrow Search Algorithm

The sparrow search algorithm (SSA), a cutting-edge swarm intelligence optimization technique introduced in 2020 [25], draws inspiration from the foraging and evasion strategies exhibited by sparrows in their natural habitat.

In regard to the SSA, the more adapted producers are the first to acquire food in a search and are responsible for discovering food for the entire sparrow colony and directing the foraging direction of all the scroungers, which gives them a broader search range. The location is updated as:

$$X_{i,j}^{t+1} \begin{cases} X_{i,j}^{t} \cdot \exp(\frac{-i}{\alpha \cdot T_{\max}}) & \text{if } Wa < Sa \\ X_{i,j}^{t+1} + Od \cdot M & \text{if } Wa \geq Sa \end{cases} \tag{11}$$

where t is the current iteration number and $T_{\max}$ is the maximum number of iterations. The position of the ith sparrow in the jth dimension is denoted by $X_{i,j}$. Additionally, α represents a random number that falls within the range of (0, 1], while Wa and Sa, ranging from [0, 1] and [0.5, 1], respectively, signify the admonition value and the safety value. Od is a random variable, following a normal distribution. Od denotes a $1 \times d$ matrix with all the elements set to 1. When $Wa < Sa$, this means that the foraging environment is temporarily free of predators. The producers initiate a widespread search when $Wa \geq Sa$, which signifies that a few sparrows have detected the predator's presence and sounded the alarm for the entire group. Promptly, all the sparrows must flee to a secure location to forage for food.

The position update formula for scrounger is:

$$X_{i,j}^{t+1}\begin{cases} X_{i,j}^{t}\cdot\exp(\frac{X_{w}^{t}-X_{i,j}^{t}}{i^{2}}) & \text{if } i>n/2 \\ X_{b}^{t+1}\cdot\left|X_{i,j}^{t}-X_{b}^{t+1}\right|\cdot Mr\cdot Od & \text{otherwise} \end{cases} \tag{12}$$

where X_b denotes the present optimal position. X_w signifies the global worst position. The matrix A is a $1 \times d$ random matrix with randomly assigned elements of 1 or -1, updated using the formula $A^{+} = A^{\mathrm{T}}(AA^{\mathrm{T}})^{-1}$. When the ith accession, which is less adapted, exceeds $n/2$, the sparrows are extremely hungry and need to find another food source to replenish their energy.

When the sparrow becomes aware of danger, it takes defensive measures against predators that can be described by a mathematical model:

$$X_{i,j}^{t+1}\begin{cases} X_{b}^{t}+\beta\cdot\left|X_{i,j}^{t+1}-X_{i,j}^{t+1}\right| & \text{if } f_i>f_g \\ X_{i,j}^{t}+K\cdot(\frac{\left|X_{i,j}^{t}-X_{w}^{t+1}\right|}{(f_i-f_w)+\omega}) & \text{if } f_i=f_g \end{cases} \tag{13}$$

where X_b signifies the globally optimal position, while β serves as a step control parameter adhering to a normal distribution. Moreover, k ranges from $[-1, 1]$, f_i represents the fitness value of the current sparrow, f_g and f_w denote the global best and worst fitness values, respectively, and ω is a small constant to prevent division by 0. When $f_i > f_g$, the sparrow is positioned at the population's edge, making it an easy target for predators. When $f_i = f_g$, the sparrow perceives danger and must move closer to its companions to reduce the risk of predation. The direction and distance of its movement are governed by K.

4. Improved Sparrow Search Algorithm

4.1. Reverse Learning Strategy

An effective method to enhance the population diversity and search capability of swarm intelligence algorithms is the reverse learning strategy [26]. The core idea is to generate reverse individuals in the region of the current individual and select the better performing individual for the iterative course of the algorithm, after comparing the fitness of the two. By combining the initial sparrow population with the reverse-generated sparrow population and sorting them according to fitness, the N individuals with the highest fitness can be filtered out for the next round of iteration. The mathematical model is defined as:

$$x'_{i,j} = ub + lb - x_{i,j} \tag{14}$$

4.2. Levy Flight Strategy

Levy flight is used for swarm intelligent position updating to heighten the global search, accelerate the convergence rate, and enhance the efficiency of the algorithm [27]. Levy flight utilizes the random walk idea to generate irregular changes. Starting from a random location, the algorithm combines high-frequency short-range search and low-frequency long-range search by jump marching and traversing. Longer steps in the early stages increase population diversity and shorter steps in the later stages accelerate algorithm convergence. This method introduces more pronounced perturbations, dispersing individuals widely across the search space in a comprehensive quest for the optimal solution, thereby enhancing the algorithm's capability to find global optima. The computational formula is:

$$Levy = \frac{\theta}{|\delta|^{1/\beta}} \tag{15}$$

where $\beta = 1.5$, θ and δ conform to a normal distribution:

$$\theta \sim N(0, \partial_u^2), \delta \sim N(0, \partial_v^2) \tag{16}$$

$$\partial_u = \left\{ \frac{\Gamma(1+\beta)\sin(\pi\beta/2)}{\Gamma[(1+\lambda)/2]\beta \cdot 2^{(\beta-1)2}} \right\}^{1/\beta}, \partial_v = 1 \tag{17}$$

where Γ is the gamma function. The ISSA producer improvement formula is:

$$X_{i,j}^{t+1} \begin{cases} Levy \cdot X_{i,j}^{t} \cdot \exp(\frac{-i}{\alpha \cdot T_{\max}}) & \text{if } Wa < Sa \\ X_{i,j}^{t+1} + Od \cdot M & \text{if } Wa \geq Sa \end{cases} \tag{18}$$

4.3. Cauchy Mutation

Cauchy mutation reinforces the efficiency of the swarm intelligence search, improves global optimization, and enhances group diversity [28,29]. During foraging, scroungers forage in the vicinity of the greatest producers and food competition can occur in an effort to become the new producers. To prevent the algorithm from becoming stuck in a local optimum, the scrounger update formula introduces a Cauchy mutation strategy to improve the global optimality of the search. The updated position of the new scrounger is:

$$X_{i,j}^{t+1} = X_b(t) + cauchy(0,1) + X_b(t) \tag{19}$$

where the standard Cauchy distribution function is *cauchy*(0,1). The Cauchy mutation function in one dimension is centered at the origin:

$$f(x) = \frac{1}{\pi}\left(\frac{1}{x^2+1}\right), -\infty < x < \infty \tag{20}$$

The flowchart illustrating the ISSA is Figure 2.

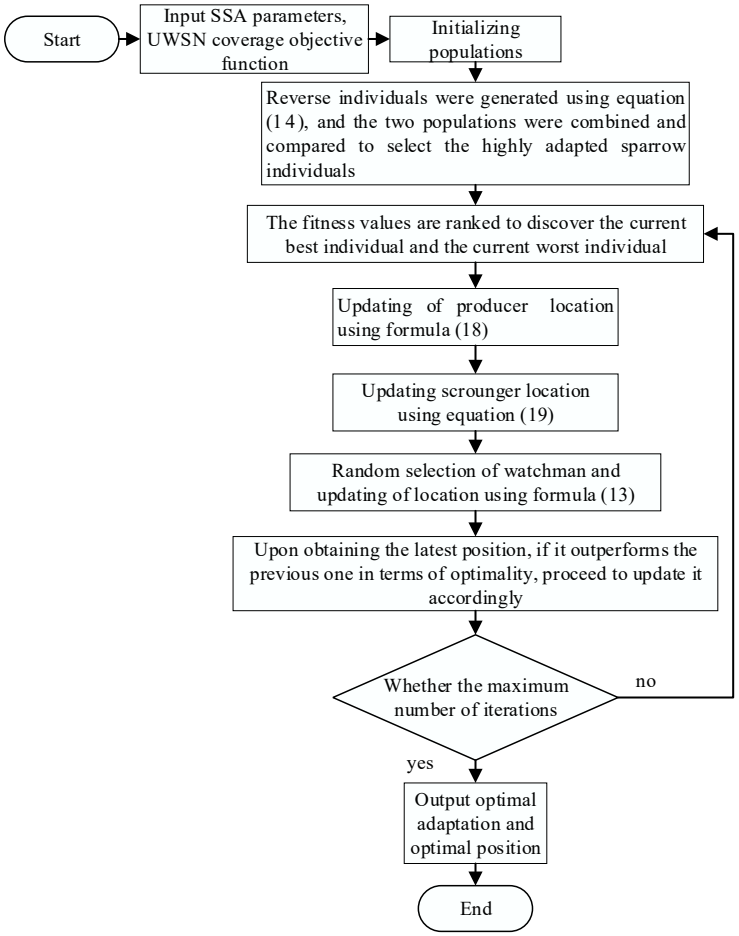


Figure 2. Flowchart of ISSA.

5. Test Function

In this study, the experimental platform used was MATLAB R2020b. To assess the ISSA algorithm's performance, F1–F4 benchmark test functions were selected and the comparison algorithms used were the basic SSA, the grey wolf optimization algorithm (GWO) [30], and the whale optimization algorithm (WOA) [31]. In order to ensure the fairness of the experimental results without interference from the parameter settings or hardware configurations, the same experimental environment was used for all the algorithms compared: 30 algorithm runs, 30 populations, and 500 iterations. The benchmark function parameters are shown in Table 1.

Table 1. Benchmark functions.

Function	Function Expression	Range of Values	Dimension	$f_{\min}$
F1	$f(x) = \sum_{i=1}^{n} x_i^2$	$[-100, 100]$	30	0
F2	$f(x) = \sum_{i=1}^{n} \lvert x_i \rvert + \prod_{i=1}^{n} \lvert x_i \rvert$	$[-10, 10]$	30	0
F3	$f(x) = \sum_{i=1}^{n} (\sum_{j=1}^{j} x_j)^2$	$[-100, 100]$	30	0
F4	$f(x) = \max_i\{\lvert x_i \rvert, 1 \le i \le n\}$	$[-100, 100]$	30	0

As shown in Figure 3 and Table 2, compared with the other algorithms, the ISSA algorithm performs better in terms of the convergence effect and is also able to search for the optimal value first, demonstrating the best search optimality. The mean and standard deviation of the ISSA are 0, which fully demonstrates the higher accuracy and stronger stability of the ISSA.

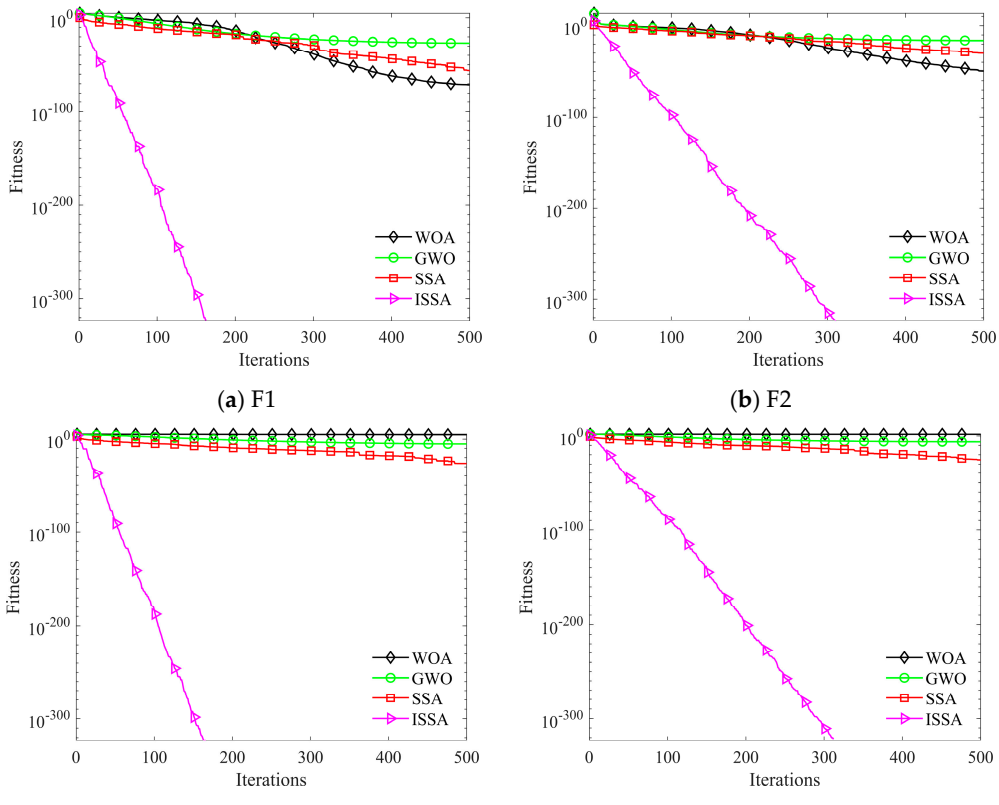


Figure 3. Benchmark test function convergence curve.

Table 2. Benchmark function results.

Function	Arithmetic	Average Value	Standard Deviation
F1	WOA	6.2569×10^{-72}	2.637×10^{-71}
	GWO	1.7863×10^{-27}	2.9902×10^{-27}
	SSA	6.0752×10^{-57}	3.3155×10^{-56}
	ISSA	0	0
F2	WOA	3.4481×10^{-50}	1.7559×10^{-49}
	GWO	8.4949×10^{-17}	6.0121×10^{-17}
	SSA	9.4539×10^{-31}	5.1019×10^{-30}
	ISSA	0	0
F3	WOA	41,539.3672	14,116.0376
	GWO	4.7859×10^{-6}	8.5759×10^{-6}
	SSA	5.1089×10^{-27}	2.7839×10^{-26}
	ISSA	0	0
F4	WOA	55.1973	24.3664
	GWO	7.3982×10^{-7}	6.3864×10^{-7}
	SSA	3.5011×10^{-26}	1.9176×10^{-25}
	ISSA	0	0

According to the benchmark function test results, it is shown that the reverse learning strategy enhances the diversity of the population, and the Levy flight and Cauchy mutation significantly enhance the local and global exploration capability of the algorithm, making the ISSA more advantageous in regard to the F1–F4 test functions.

6. Marine Ranching UWSNs Coverage Experiment

To roundly validate the efficiency gains of the ISSA for UWSNs node coverage, the fundamental SSA, WOA, and GWO were chosen for comparison. As depicted in Table 3, the experimental parameters were set. The experiments were mainly carried out to assess the node deployment, node energy consumption, coverage with a different number of mobile nodes, and AUV node obstacle avoidance. By conducting experiments under such conditions, the performance of the algorithm can be more comprehensively evaluated in a variety of different situations.

Table 3. Experimental parameters.

Parameter Name	Parameter Value
Simulation area	50 m × 50 m × 50 m
Total number of sensor nodes/N	50
Mobile nodes/m	10–35
Perceptual radius/R	10
Communication radius/Rc	20
Population size/pop	30
Iterations/$T_{\max}$	500

6.1. Node Deployment

In this experiment, 35 mobile nodes and 15 fixed nodes were set up, and Figure 4 shows the classification of the nodes, with red spheres for the fixed node sensing range and light blue spheres for the mobile node sensing range. Figures 5–9 illustrate the node coverage outcomes achieved by the four algorithms. During the initial deployment stage, the nodes were deployed in a randomized manner within the monitoring area. By comparing the coverage results of these four algorithms for the same conditions, their performance differences in regard to real applications can be evaluated more intuitively. Figures 5–9 show the initial deployment, WOA deployment, GWO deployment, SSA deployment, and ISSA deployment, respectively. Figure 10 shows the coverage curve of each algorithm.

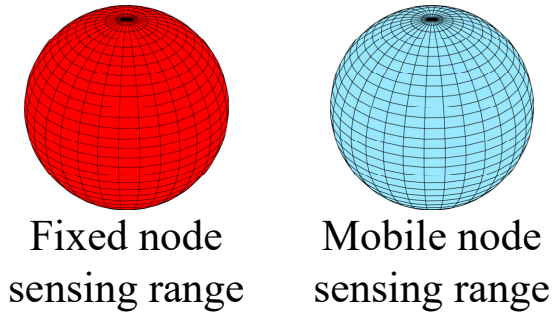


Figure 4. Node classification.

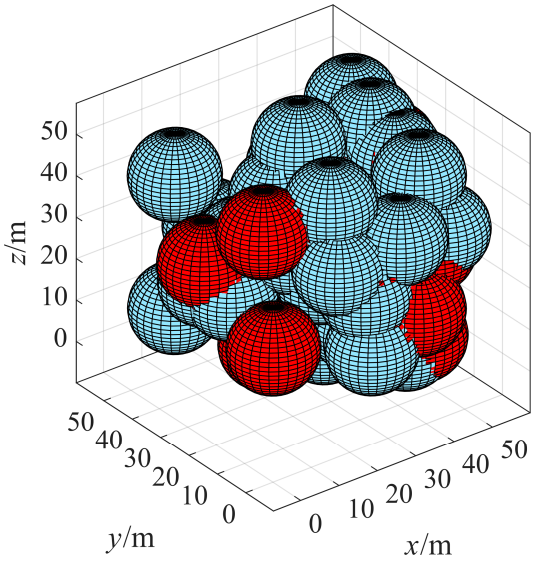


Figure 5. Initial deployment.

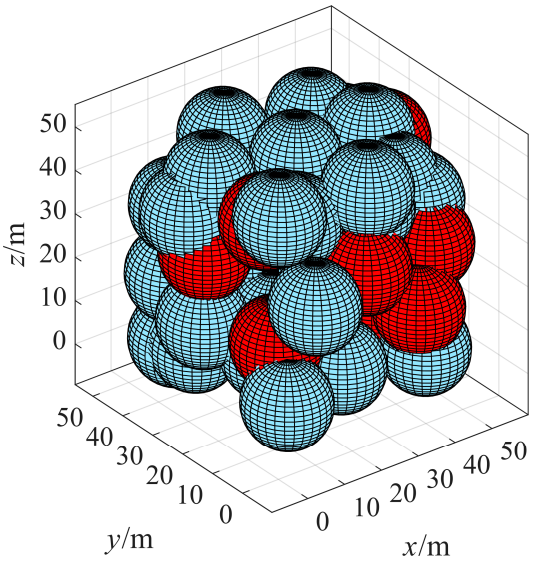


Figure 6. WOA deployment.

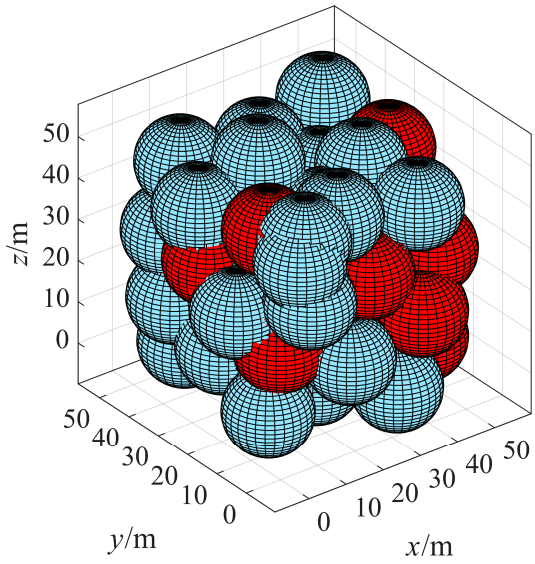


Figure 7. GWO deployment.

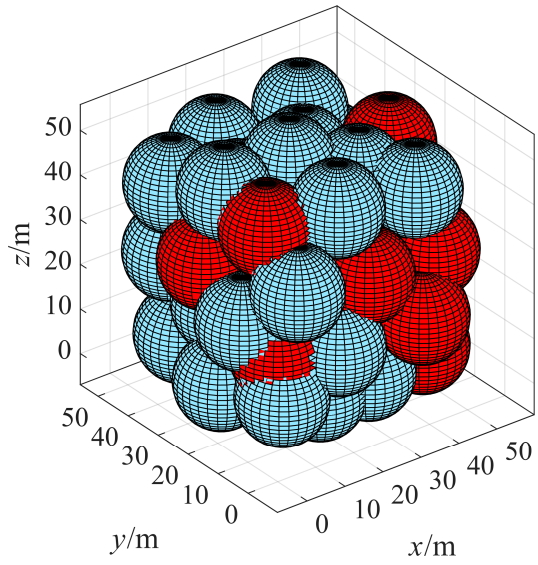


Figure 8. SSA deployment.

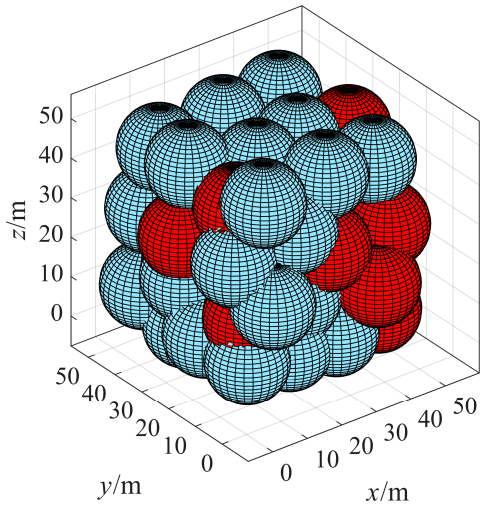


Figure 9. ISSA deployment.

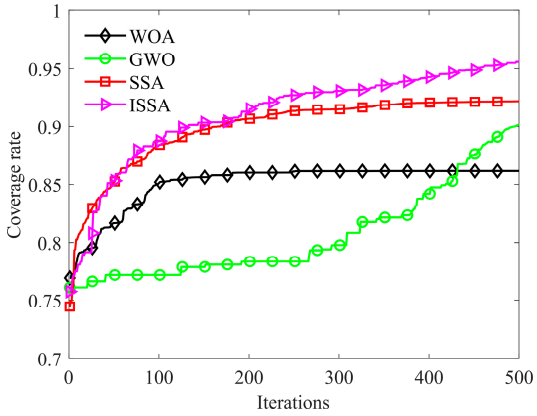


Figure 10. Coverage of each algorithm.

Based on the deployment graphs in Figures 5–9, it is evident that the ISSA deployment is the most effective, with fewer coverage holes and more uniform node coverage. The coverage is improved to a great extent, especially when compared to the initial coverage. The coverage of each algorithm is obtained according to Figure 10, where ISSA coverage is 95.59%, SSA coverage is 92.17%, GWO coverage is 90.11%, WOA coverage is 86.17%, and the initial coverage is 75.03%.

6.2. Node Energy Consumption

The range of activity carried out by nodes deployed underwater is strongly constrained by the battery energy. Whenever the distance traveled by a node increases, its energy consumption also rises. Therefore, while performing monitoring tasks, it is necessary to ensure the efficient execution of the task and the long-lasting operation of the nodes. Figure 11 shows the distance traveled by the mobile nodes for each algorithm.

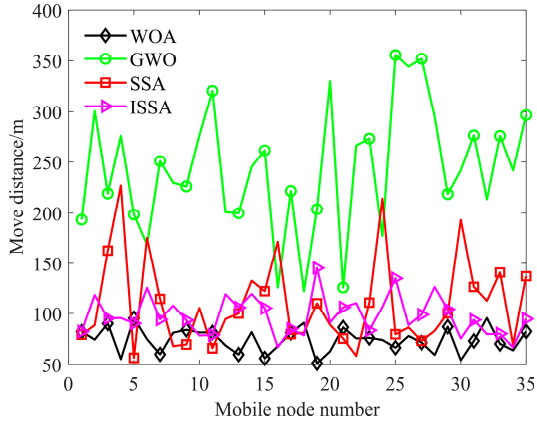


Figure 11. Moving distance of mobile nodes for each algorithm.

According to the results in Figure 11, the WOA node moves the shortest distance, which is due to the fact that the WOA finds the global optimum earlier and the node position is no longer moving to find the optimal position. The ISSA moves the second shortest distance and achieves greater coverage, with a shorter node-moving distance.

As a mobile node, the AUV consumes energy when searching for the best deployment location. The electricity consumption of the AUV is set to 0.0272 kWh/km in the experiment. The total energy consumption of the nodes is calculated based on this AUV energy consumption parameter.

As shown in Figure 12, the electricity consumption of the ISSA is 0.0931 kWh, which is the second largest, which fully proves the advantages of the proposed method in terms of energy consumption.

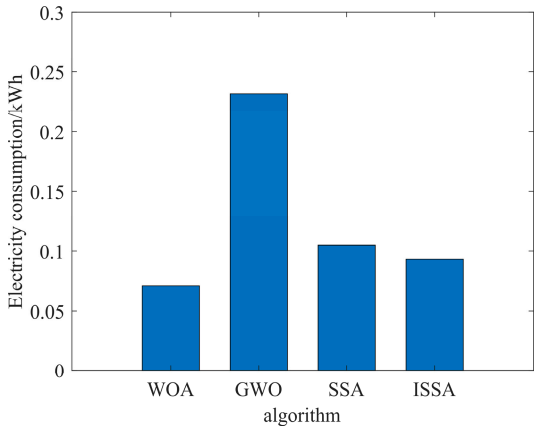


Figure 12. The total electricity consumption of each algorithm.

6.3. Coverage of Various Quantities of Mobile Nodes

This experiment verifies the coverage comparison of the quantities of mobile nodes. When deploying UWSNs nodes in marine ranching, the quantity of mobile nodes can be selected based on the construction cost to fully meet the monitoring requirements. Figure 13 displays the rate of coverage achieved by each algorithm with varying quantities of mobile nodes.

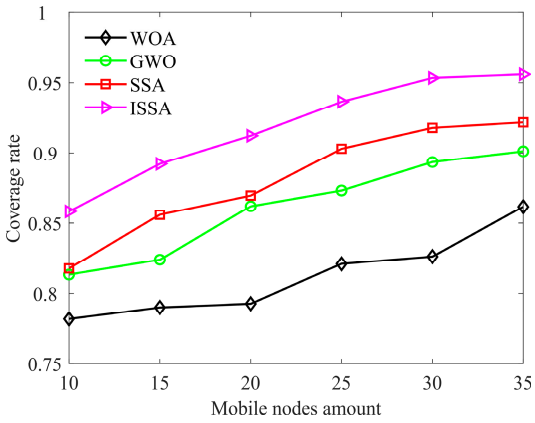


Figure 13. Coverage of the number of mobile nodes for each algorithm.

According to the results in Figure 13, the coverage is improved with the increase in the number of mobile nodes for each algorithm. Among them all, ISSA coverage is higher than the other three algorithms.

6.4. AUV Node Obstacle Avoidance

After the nodes were deployed, the coverage area still has coverage holes, due to water currents, underwater noise, and other effects. In the area of fast water current, the communication interference is large and the sensor monitoring signal is unstable. At this time, the AUV needs to move to the area where the monitoring signal is unstable or to where the coverage hole appears to complete the monitoring task. During the navigation task, the AUV applies the algorithms mentioned in the experiment to identify obstacles, avoid them, and explore the best navigation path. Figure 14 displays the underwater navigation path and Figure 15 displays the top view of the underwater navigation path for each algorithm.

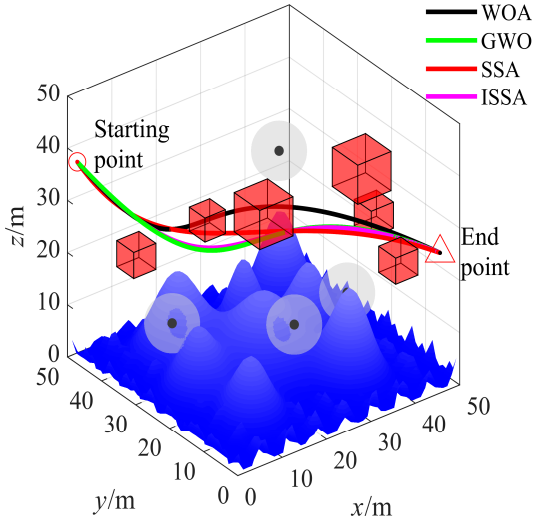


Figure 14. Underwater navigation path for each algorithm.

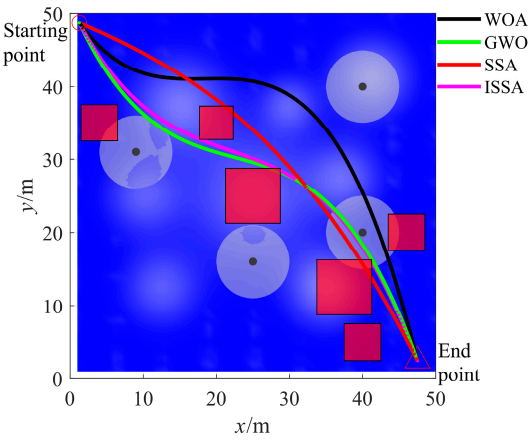


Figure 15. Top view of underwater navigation path for each algorithm.

According to Figures 14 and 15, the ISSA path length is shorter than the other algorithms when performing the obstacle avoidance task, and the shorter the path length, the lower the energy usage. Under these circumstances, the ISSA path length is 72.95 m, the SSA is 73.23 m, the GWO is 73.43 m, and the WOA is 78.74 m.

7. Conclusions

To address the challenges in deploying sensor nodes in complex 3D underwater environments for marine ranching, a UWSNs coverage method, based on the ISSA, is proposed. The SSA is enhanced by incorporating the reverse learning strategy, Levy flight, and Cauchy mutation, thus realizing more efficient UWSNs coverage. In the benchmark function, the ISSA's performance was superior in terms of the four tested functions. When nodes are deployed underwater, an AUV is used to find the best location for complete coverage of the task. After the node completes the first deployment, when there is a monitoring hole in the network, the AUV moves again to the area that needs to be monitored for the task. The simulation experiments show that the proposed ISSA has higher coverage than other swarm intelligence algorithms and less energy consumption by the nodes.

The ISSA falls into the global optimum at a later stage when the nodes are deployed and has limited ability to further improve the coverage. In future work, the SSA will be continuously improved to enhance the optimal search capability and more complex marine environments will be simulated during simulation experiments, including different

water depths, current speeds, and obstacle distributions, etc., in order to comprehensively evaluate the adaptability and superiority of the ISSA in practical applications.

Author Contributions: Conceptualization, L.F. and J.W.; methodology, L.F.; software, L.F.; validation, L.F. and J.W.; formal analysis, L.F.; investigation, L.F.; resources, J.W.; data curation, L.F.; writing—original draft preparation, L.F.; writing—review and editing, J.W; visualization, L.F.; supervision, J.W.; project administration, L.F.; funding acquisition, J.W. All authors have read and agreed to the published version of the manuscript.

Funding: This research was funded by the Special Project on New Generation Information Technology in Key Areas of General Universities in Guangdong Province, grant number 2020ZDZX3008.

Data Availability Statement: Where data is unavailable due to privacy or ethical restrictions. Data are not publicly available, please contact the authors for experimental methods and details.

Conflicts of Interest: The authors declare no conflict of interest.

References

1. Kandris, D.; Nakas, C.; Vomvas, D.; Koulouras, G. Applications of Wireless Sensor Networks: An Up-to-Date Survey. *Appl. Syst. Innov.* **2020**, *3*, 14. [CrossRef]
2. Yu, J.; Zhang, L. Evolution of marine ranching policies in China: Review, performance and prospects. *Sci. Total Environ.* **2020**, *737*, 139782. [CrossRef] [PubMed]
3. Luo, C.; Wang, B.; Cao, Y.; Xin, G.; He, C.; Ma, L. A hybrid coverage control for enhancing UWSN localizability using IBSO-VFA. *Ad Hoc Netw.* **2021**, *123*, 102694. [CrossRef]
4. Kuang, Y.; Jiang, B.; Cui, X.; Li, S.; Wang, J.; Song, H. Adaptive double-loop coverage optimization of underwater wireless directional restricted sensor networks. *Ad Hoc Netw.* **2024**, *156*, 103409. [CrossRef]
5. Ghannadrezaii, H.; Bousquet, J.-F. Maximizing network coverage in a multichannel short-range underwater acoustic sensor network. *Comput. Netw.* **2019**, *160*, 1–10. [CrossRef]
6. Zhang, Q.; Fok, M.P. A two-phase coverage-enhancing algorithm for hybrid wireless sensor networks. *Sensors* **2017**, *17*, 117. [CrossRef]
7. Simionato, G.; Cimino, M.G. Swarm intelligence for hole detection and healing in wireless sensor networks. *Comput. Netw.* **2024**, *250*, 110538. [CrossRef]
8. Dong, M.; Li, H.; Qin, Y.; Hu, Y.; Huang, H. A secure and accurate localization algorithm for mobile nodes in underwater acoustic network. *Eng. Appl. Artif. Intell.* **2024**, *133*, 108157. [CrossRef]
9. Cai, W.; Liu, Z.; Zhang, M.; Wang, C. Cooperative Artificial Intelligence for underwater robotic swarm. *Robot. Auton. Syst.* **2023**, *164*, 104410. [CrossRef]
10. Li, Y.; Zhao, L.; Wang, Y.; Wen, Q. Improved sand cat swarm optimization algorithm for enhancing coverage of wireless sensor networks. *Measurement* **2024**, *233*, 114649. [CrossRef]
11. Yan, Z.; Yan, J.; Wu, Y.; Cai, S.; Wang, H. A novel reinforcement learning based tuna swarm optimization algorithm for autonomous underwater vehicle path planning. *Math. Comput. Simul.* **2023**, *209*, 55–86. [CrossRef]
12. Li, Y.; Yao, Y.; Hu, S.; Wen, Q.; Zhao, F. Coverage Enhancement Strategy for WSNs Based on Multi-Objective Ant Lion Optimizer. *IEEE Sens. J.* **2023**, *23*, 13762–13773. [CrossRef]
13. Yao, Y.; Hu, S.; Li, Y.; Wen, Q. A node deployment optimization algorithm of WSNs based on improved moth flame search. *IEEE Sens. J.* **2022**, *22*, 10018–10030. [CrossRef]
14. Chen, H.; Wang, X.; Ge, B.; Zhang, T.; Zhu, Z. A multi-strategy improved sparrow search algorithm for coverage optimization in a WSN. *Sensors* **2023**, *23*, 4124. [CrossRef] [PubMed]
15. Ou, Y.; Qin, F.; Zhou, K.-Q.; Yin, P.-F.; Mo, L.-P.; Mohd Zain, A. An Improved Grey Wolf Optimizer with Multi-Strategies Coverage in Wireless Sensor Networks. *Symmetry* **2024**, *16*, 286. [CrossRef]
16. Chang, Y.; He, D.; Qu, L. An improved tuna swarm optimization algorithm based on behavior evaluation for wireless sensor network coverage optimization. *Telecommun. Syst.* **2024**, *86*, 829–851. [CrossRef]
17. Zhang, Y.; Wang, M.; Liang, J.; Zhang, H.; Chen, W.; Jiang, S. Coverage enhancing of 3D underwater sensor networks based on improved fruit fly optimization algorithm. *Soft Comput.* **2017**, *21*, 6019–6029. [CrossRef]
18. Priyadarshi, R.; Gupta, B. Area coverage optimization in three-dimensional wireless sensor network. *Wirel. Pers. Commun.* **2021**, *117*, 843–865. [CrossRef]
19. Yu, X.; Duan, Y.; Cai, Z.; Luo, W. An adaptive learning grey wolf optimizer for coverage optimization in WSNs. *Expert Syst. Appl.* **2024**, *238*, 121917. [CrossRef]
20. Wang, W.; Huang, H.; He, F.; Xiao, F.; Jiang, X.; Sha, C. An enhanced virtual force algorithm for diverse k-coverage deployment of 3D underwater wireless sensor networks. *Sensors* **2019**, *19*, 3496. [CrossRef]
21. Saad, A.; Senouci, M.R.; Benyattou, O. Toward a realistic approach for the deployment of 3D Wireless Sensor Networks. *IEEE Trans. Mob. Comput.* **2020**, *21*, 1508–1519. [CrossRef]

22. Luo, C.; Cao, Y.; Xin, G.; Wang, B.; Lu, E.; Wang, H. Three-dimensional coverage optimization of underwater nodes under multiconstraints combined with water flow. *IEEE Internet Things J.* **2021**, *9*, 2375–2389. [CrossRef]
23. Liu, N.; Chai, Q.-W.; Liu, S.; Zheng, W.-M. A novel compact particle swarm optimization for optimizing coverage of 3d in wireless sensor network. *Wirel. Commun. Mob. Comput.* **2022**, *2022*, 4600787. [CrossRef]
24. Gou, P.; Guo, B.; Guo, M.; Mao, S. VKECE-3D: Energy-efficient coverage enhancement in three-dimensional heterogeneous wireless sensor networks based on 3D-voronoi and K-means algorithm. *Sensors* **2023**, *23*, 573. [CrossRef]
25. Xue, J.; Shen, B. A novel swarm intelligence optimization approach: Sparrow search algorithm. *Syst. Sci. Control Eng.* **2020**, *8*, 22–34. [CrossRef]
26. Sharma, A.; Sharma, A.; Averbukh, M.; Rajput, S.; Jately, V.; Choudhury, S.; Azzopardi, B. Improved moth flame optimization algorithm based on opposition-based learning and Lévy flight distribution for parameter estimation of solar module. *Energy Rep.* **2022**, *8*, 6576–6592. [CrossRef]
27. Zhang, J.; Li, L.; Zhang, H.; Wang, F.; Tian, Y. A novel sparrow search algorithm with integrates spawning strategy. *Clust. Comput.* **2024**, *27*, 1753–1773. [CrossRef]
28. Liang, J.; Tian, M.; Liu, Y.; Zhou, J. Coverage optimization of soil moisture wireless sensor networks based on adaptive Cauchy variant butterfly optimization algorithm. *Sci. Rep.* **2022**, *12*, 11687. [CrossRef]
29. Wang, S.; Cao, L.; Chen, Y.; Chen, C.; Yue, Y.; Zhu, W. Gorilla optimization algorithm combining sine cosine and cauchy variations and its engineering applications. *Sci. Rep.* **2024**, *14*, 7578. [CrossRef]
30. Mirjalili, S.; Mirjalili, S.M.; Lewis, A. Grey wolf optimizer. *Adv. Eng. Softw.* **2014**, *69*, 46–61. [CrossRef]
31. Mirjalili, S.; Lewis, A. The whale optimization algorithm. *Adv. Eng. Softw.* **2016**, *95*, 51–67. [CrossRef]

Disclaimer/Publisher's Note: The statements, opinions and data contained in all publications are solely those of the individual author(s) and contributor(s) and not of MDPI and/or the editor(s). MDPI and/or the editor(s) disclaim responsibility for any injury to people or property resulting from any ideas, methods, instructions or products referred to in the content.